Optimal capacity configuration of a wind-solar-battery-diesel microgrid system using continuous grey wolf optimization

Zhiling Ren[a,b], Qinwen Yu[a], Dong Lin[a,c], Yun Dong[a,c,*]

[a] *Faculty of Electrical and Control Engineering, Liaoning Technical University, Huludao 125100, China*
[b] *Ordos Institute of Liaoning Technical University,Ordos 017000,China*
[c] *Department of Electrical, Electronic and Computer Engineering, University of Pretoria, Pretoria 0002, South Africa*

Abstract

This study presents a novel optimization method for the design of a hybrid microgrid system, consisting of wind turbines, photovoltaic systems, battery energy storage systems, and diesel generators. A Continuous Grey Wolf Optimization (CGWO) algorithm is proposed to tackle the challenges of nonlinearity and stochastic disturbances in the system's capacity configuration. The CGWO enhances the traditional Grey Wolf Optimization (GWO) by incorporating an improved convergence factor and a dynamic weighting strategy, significantly increasing convergence speed and solution quality. A case study is conducted to evaluate four power supply schemes for the microgrid. Results indicate that Scheme 3 achieves the lowest total cost and environmental conversion expenses, with reductions of 30.12% and 59.7% compared to Scheme 1, and 16.74% and 39.84% compared to Scheme 2, respectively. In addition, the CGWO reduces diesel generator usage by 23.78% compared to the GWO and 22.04% compared to Particle Swarm Optimization (PSO), while decreasing power shortages by 62.09% and 60.25%, respectively. These findings highlight the CGWO's effectiveness in optimizing microgrid configurations, balancing cost, sustainability, and reliability. The proposed method provides valuable insights for designing cost-efficient and environmentally sustainable energy systems.

Keywords: Microgrid system, Capacity configuration, Continuous grey wolf optimization, Environmental cost, Sustainable energy systems

1. Introduction

Promoting renewable energy utilization and reducing dependence on fossil fuels have become global imperatives [1]. However, in remote areas, diesel power generation faces significant challenges, including high operational costs, fuel price volatility, and environmental pollution, which collectively hinder the stability of electricity supply. In contrast, these regions often possess abundant renewable energy resources, such as wind and solar energy. As a result, developing microgrids centered around renewable energy has emerged as a vital component of future smart grids [2]. In the planning and design of microgrids, optimizing the capacity configuration of hybrid microgrid systems by effectively utilizing natural resources has become a core challenge. Existing research on microgrid capacity optimization, for both standalone and grid-connected systems, primarily focuses on two key aspects: the development of objective functions and the exploration of solution methods [3, 4].

In the study of objective functions, Zhang et al. [5] proposed an optimal configuration method for distributed generation equipment in DC microgrids to enhance economic performance. This method considers system operation modes and objectives, analyzing various constraints, operational schemes, and economic goals. To ensure reliable power supply, integrating energy storage systems (ESS) into microgrids is essential. Research on ESS capacity configuration primarily focuses on investment costs and supply reliability [6, 7]. When determining storage capacity based on costs, researchers typically account for the lifecycle income and associated expenses of power stations [8, 9], as well as the comprehensive operational costs of photovoltaic (PV) storage systems [10, 11]. Huang et al. [12] proposed a hierarchi-

*Corresponding author
Email address: yundong713@163.com (Yun Dong)

Nomenclature

a	Intercept coefficient	A	Coefficient vector
b	Slope coefficient	C	Coefficient vector
C_{ini}	Annual initial investment cost (CNY)	C_m	Annual maintenance cost (CNY)
C_{er}	Annual equipment replacement cost (CNY)	C_{fuel}	Fuel cost (CNY/L)
C_{pol}	Environmental cost (CNY)	D_i	Distances from wolves to the prey
f_{ewr}	Energy wastage rate	f_{lps}	Load shedding probability
G	Solar irradiance (W/m^2)	G_n	Reference solar irradiance (W/m^2)
K_i	Operation and maintenance cost coefficient	K_{fuel}	Diesel price (CNY)
K_{crf}	Capital recovery factor	K_{sff}	Sunk fund factor
K_i^{γ}	Emission coefficient for i_{th} pollutant	P_L	Load power at time step t (kW)
P_i	Rated capacity of i_{th} micro-source (kW)	P_{dch}	Battery discharging power (kW)
P_{ch}	Battery charging power (kW)	P_n	Rated output power of photovoltaic (kW)
P_{wt}	Wind turbine generated power (kW)	P_{pv}	Photovoltaic power (kW)
E_s	Battery storage capacity (kW)	P_{bre}	Power shortage (kW)
$\mathrm{P_{dis,max}}$	Battery maximum discharging efficiency (kW)	$\mathrm{P_{cha,max}}$	Battery maximum charging efficiency (kW)
$\mathrm{P_{dg,min}}$	Minimum power of per diesel generator (kW)	$\mathrm{P_{dg,max}}$	Maximum power of per diesel generator (kW)
P_{dg}	Actual power output of the diesel generator (kW)	P_1	Photovoltaic power supply to the load (kW)
P_2	Wind turbine power supply to the load (kW)	P_3	Battery power supply to the load (kW)
P_4	Diesel generator power supply to the load (kW)	P_5	Photovoltaic power used for battery charging (kW)
P_6	Wind turbine power used for battery charging (kW)	r	Bank interest rate
R_i	Replacement cost of i_{th} micro-source (CNY)	SOC	State of charge of battery
s	Salvage value coefficient	T_c	Surface temperature (℃)
T_r	PV panel temperature (℃)	v	Actual wind speed (m/s)
v_n	Rated wind speed (m/s)	v_{ci}	Cut-in speed (m/s)
v_{co}	Cut-out speed (m/s)	V_i	Treatment cost for emission of i_{th} pollutant (CNY)
X^{wt}	Number of wind turbines	X^{PV}	Number of PV panels
X^b	Number of batteries	X^{dg}	Number of diesel generators
X_p	Position vector of the prey	X_i	Positions of wolves determined by D_i
Y_i	Lifetime of i_{th} micro-source	λ	Temperature coefficient
ξ	Self-discharge rate	η_i	Inverter coefficient
η_s	charge-discharge conversion rate of the battery	η_r	Rectification coefficient
α	Highest-ranking wolf	β	Subordinate wolf to α
δ	Obeys the commands of α and β	ω	Lowest-ranking wolf

cal design method for distributed batteries that significantly reduces battery capacity and sharing process losses, thereby improving energy efficiency and flexibility in positive energy communities. Similarly, Nazir et al. [13] developed a storage capacity configuration method based on reliable output power to address the intermittency of renewable energy. Through cost-benefit analysis, they suggested an approach for determining the optimal ESS capacity by considering reliable output power. Diab et al. [14] further explored this area by formulating an optimization objective function aimed at minimizing costs, the probability of power supply loss, and virtual load. Simulation results from microgrid operations demonstrated that optimized configurations improve reliability but come at the expense of increased investment costs.

In solving optimization problems, the integration of diverse distributed energy resources in microgrids results in significantly different output characteristics, leading to highly nonlinear, complex, and uncertain capacity optimization challenges [15, 16]. Traditional optimization methods, such as mathematical programming, often struggle with escaping local optima and addressing nonlinearity, underscoring the need for advanced algorithms to achieve efficient and economical microgrid capacity configurations [17, 18]. The use of meta-heuristic algorithms for optimizing standalone microgrid configurations has gained widespread attention [19, 20]. These algorithms mimic natural behaviors to avoid local optima, enabling efficient solutions to complex optimization problems [21]. For example, Yang et al. [22] proposed an innovative approach that addresses the inherent limitations of traditional optimization techniques, which often fail to achieve optimal results due to system complexities. Similarly, Yildiz et al. [23] emphasized the critical need for continuous improvement in traditional methods to handle real-world applications effectively. Almadhor et al.[24] elaborated on the working principles of the Particle Swarm Optimization (PSO) and Bat algorithms, introducing the design rationale of the Bat Algorithm-Particle Swarm

Optimization (BAPSO) algorithm. By incorporating the frequency parameter of the Bat algorithm into the velocity update equation of the PSO algorithm, BAPSO combines the strengths of both methods, achieving faster convergence and improved optimization of energy system capacities. Additionally, Hossain et al. [25] introduced a PSO algorithm with an improved cost function for real-time energy management in converter-based microgrids, enhancing energy efficiency. Further advancements include hybrid optimization methods, such as the Particle Swarm Optimization-Grey Wolf Optimization (PSO-GWO) algorithm proposed by Gourav et al. [26], which was applied to optimize the configuration of rural microgrids in Bihar, India. This hybrid algorithm was utilized to optimize the objective function and demonstrated superior performance compared to other algorithms, such as teaching-learning-based optimization.

The power capacity configuration of standalone microgrids is a critical component of system optimization design and serves as the foundation for ensuring safe and reliable system operation [27]. The diversity of distributed generation sources in standalone microgrids, coupled with significant variations in the output characteristics of individual units, makes the optimization of microgrid capacity highly nonlinear, complex, and uncertain. This inherent complexity often prevents traditional optimization methods from achieving satisfactory results [28]. Despite extensive research on microgrid capacity configuration, there remains a lack of comprehensive integration between operational control strategies and solution algorithms [29]. Effective optimization of microgrid capacity requires not only refined control strategies but also advanced algorithms capable of addressing the complexity and uncertainty of the system [30]. To bridge this gap, future research must focus on developing holistic approaches that integrate optimized control strategies, establish more comprehensive objective functions and constraints, and employ more efficient and precise optimization algorithms.

This paper proposes a method for optimizing the capacity configuration of a wind-solar-battery-diesel microgrid using the Continuous Grey Wolf Optimization (CGWO) algorithm. Traditional Grey Wolf Optimization (GWO) algorithms often suffer from slow convergence speeds and a tendency toward premature convergence, limiting their effectiveness in solving complex optimization problems [31, 32]. To address these limitations, the proposed CGWO algorithm introduces a convergence factor based on cosine law variation and incorporates dynamic weights to update the positions of the top three grey wolves. These enhancements accelerate the convergence speed and improve the solution accuracy, making the algorithm more robust and efficient for microgrid capacity optimization.

The main contributions of this study can be summarized as follows:

(1) A comprehensive optimization framework is proposed for configuring the capacities of microgrids that integrate wind turbines (WT), PV, battery energy storage systems (BESS), and diesel generators (DG). The framework addresses operational constraints, environmental considerations, and reliability requirements while minimizing total annual costs.

(2) This study introduces CGWO, an enhanced version of the traditional GWO algorithm. By incorporating a cosine-law-based convergence factor and a dynamic weighting strategy, CGWO achieves improved convergence speed, solution accuracy, and the ability to handle complex, multimodal optimization problems.

(3) The proposed CGWO algorithm is rigorously validated through benchmark testing on CEC2005 functions, demonstrating superior performance over GWO in addressing complex optimization challenges. Additionally, its application to a standalone hybrid microgrid system highlights its potential for improving operational efficiency and sustainability.

(4) The CGWO algorithm is applied to analyze and optimize different power supply schemes for microgrids. Among the schemes evaluated, the framework identifies the most cost-effective configuration, enhancing renewable energy utilization and reducing dependence on fossil fuels.

The rest of the paper is organized as follows: Section 2 provides a comprehensive overview of the microgrid system, and design considerations. Section 3 formulates the optimization problem for microgrid capacity configuration, detailing the objective function and associated constraints. Section 4 introduces the CGWO algorithm, including benchmark testing and explaining its key enhancements and implementation details. Section 5 presents the simulation results, featuring a case study on hybrid microgrid systems and a comparative analysis of various algorithms. Finally, Section 6 concludes the paper with a summary of findings and suggestions for future research directions.

2. System description

In this paper, the hybrid microgrid system consists of WTs, PV panels, battery energy storage systems, DGs, inverters, and loads [33]. A DC bus networking method is chosen for its advantages, such as simple control and easy scalability, based on the characteristics of various networking methods of the wind-solar-battery-diesel microgrid system [34, 35]. The system structure is shown in Figure 1, which illustrates a microgrid system integrating renewable energy generation from WTs and PV panels, energy storage systems, and DGs. The system is designed to supply power to residential, commercial, and industrial loads. It includes components such as DC/DC converters, DC/AC inverters, and AC/DC converters, ensuring the seamless transmission and conversion of electricity between various power sources and loads.

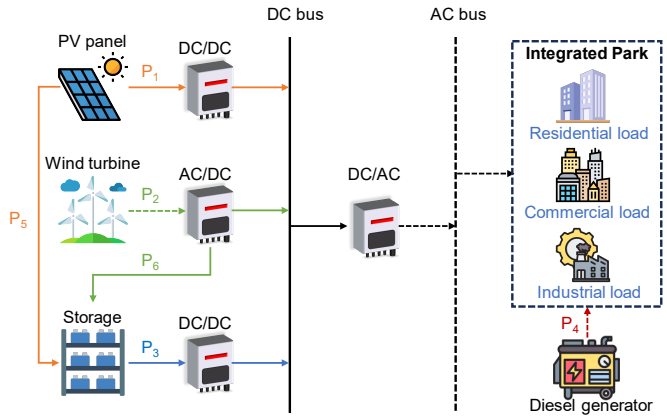

Figure 1: Microgrid system architecture diagram

2.1. Wind turbine generation model

The output power of wind power is primarily related to wind speed, and the changes in wind speed follow the Weibull distribution [36], from which the wind power output power model is as follows:

$$P_{wt} = \begin{cases} 0, & v < v_{ci}, \\ P_n \frac{v - v_{ci}}{v_n - v_{ci}}, & v_{ci} \le v < v_n, \\ P_n, & v_n \le v < v_{co}, \\ 0, & v_{co} \le v, \end{cases} \tag{1}$$

where P_{wt} and v correspond to the actual output power and actual wind speed of the WT; P_n and v_n are the rated output power and rated wind speed of the WT; v_{ci} and v_{co} are the cut-in and cut-out wind speeds.

2.2. Photovoltaic power generation model

The model for PV output power, as described in reference [37], is as follows:

$$P_{pv} = P_n \frac{G}{G_n} \left(1 + \lambda \left(T_c - T_r\right)\right), \tag{2}$$

where P_{pv} represents the output power of the PV panels; G is the solar irradiance W/m^2; the reference solar irradiance G_n is set at 1000W/m^2; the temperature T_r of the PV panel is 25°C; T_c is surface temperature; P_n is the nominal power of the PV panel; λ is the temperature coefficient, with a value of -0.0047.

2.3. Energy storage model

In an independent hybrid energy microgrid, the battery bank acts as a charging/discharging energy storage device, mainly achieving a balanced power supply load and energy buffering distribution[38]. The state of charge (SOC) of the BESS at time t is described during charging and discharging processes.

$$SOC(t) = \begin{cases} (1-\xi)\, SOC(t-1) - \frac{P_{dch}(t)}{P_s \eta_s} \times 100\%, \\ (1-\xi)\, SOC(t-1) + \frac{P_{ch}(t)\, \eta_s}{P_s} \times 100\% \end{cases} \tag{3}$$

where $P_{dch}(t)$, $P_{ch}(t)$ represent the amount of charge and discharge of the battery at time t; ξ and η_s are the self-discharge rate and the charge-discharge conversion rate of the battery; $SOC(t)$ represents the state of charge of the battery at time t .

2.4. Diesel generator model

In the event of insufficient output from the hybrid energy sources, the DG set is activated as an emergency backup to meet the load demand. The mathematical model of the DG is as follows:

$$P_{dg}(t) = \begin{cases} \mathrm{P_{dg,min}}, & P_{dg}(t) < \mathrm{P_{dg,min}}, \\ P_{dg}(t), & \mathrm{P_{dg,min}} \le P_{dg}(t) < \mathrm{P_{dg,max}}, \\ \mathrm{P_{dg,max}}, & \mathrm{P_{dg,max}} \le P_{dg}(t) \end{cases} \tag{4}$$

where P_{dg} represents the actual power output of the DG, kW; $\mathrm{P_{dg,min}}$ and $\mathrm{P}_{dg,max}$ are the minimum power of per DG and maximum power of per DG, kW; $P_{dg}(t)$ represents the actual power output of the DG at time t.

3. Formulation of the microgrid capacity optimization problem

In this paper, the capacity configuration of a wind-solar-battery-diesel microgrid is optimized to rationally allocate the capacity ratios of WTs, PV panels, storage batteries, and DGs. The system aims to meet load demand and other constraints while considering both stability and economy. The annual comprehensive cost includes the system's initial investment cost, annual maintenance cost, annual equipment replacement cost, fuel cost, and environmental protection conversion cost. Stability considerations include the load loss rate and energy waste rate.

3.1. Objective function

The primary objective is to minimize the annual comprehensive cost of the hybrid microgrid system by optimizing factors such as the annualized initial investment, maintenance, equipment replacement, fuel, and environmental costs. This involves amortizing the initial investment over the system's lifespan, accounting for salvage value, and incorporating regular maintenance and replacement costs. By summing these costs and optimizing the operation, we aim to identify the most cost-effective and environmentally sustainable strategy for the microgrid. The specific cost functions for each participant are to be provided for detailed analysis.The cost function of each participant is shown as:

$$C_{all} = (1-s)C_{ini} + C_m + C_{er} + C_{fuel} + C_{pol}, \quad (5)$$

where C_{all} is annual comprehensive cost of the whole microgrid, C_{ini} represents the annual average initial investment cost, C_m is the annual maintenance cost, C_{er} is the annual equipment replacement cost, C_{fuel} is the fuel cost, C_{pol} is the environmental cost, and s is the salvage value coefficient, which is set at 5%.

3.1.1. Annual average initial investment cost

The annualized initial investment cost is a crucial economic metric in the planning and design of microgrids. It represents the annualized expense of the initial investment required for the components of the microgrid. The function for the annualized initial investment cost is as follows:

$$C_{ini} = \sum_{i=1}^{4} X^i U_i K_{crf}, \quad (6)$$

where X^i is the number of the i_{th} type of micro-source; U_i is the unit price of the i_{th} type of micro-source. K_{crf} denotes the discount rate, and its expression is:

$$K_{crf} = \frac{r(1+r)^Y}{(1+r)^Y - 1}, \quad (7)$$

where r is the bank interest rate of 4.75%, and Y is the operational lifespan of the microgrid system, which is 20 years.

3.1.2. Annual operation and maintenance cost

Annual operation and maintenance costs are incurred over the year for the regular operation and upkeep of a microgrid and its components. These costs encompass all ongoing expenses necessary to ensure the smooth operation and reliability of the microgrid.

$$C_m = \sum_{i=1}^{4} X^i K_i P_i, \quad (8)$$

where K_i is the operation and maintenance cost coefficient for the i_{th} type of micro-source, (CNY/kW); P_i is the rated capacity of a single unit of the i_{th} type of micro-source.

3.1.3. Annual equipment replacement cost

Annual equipment replacement costs are associated with the periodic replacement of worn-out or obsolete equipment within a microgrid and its components. These costs are a necessary consideration for the long-term operation of the microgrid. The function for calculating the annual equipment replacement cost is as follows:

$$C_{er} = \sum_{i=1}^{4} X^i R_i K_{sff}, \quad (9)$$

where R_i is the replacement cost for each unit of the i_{th} type of micro-source (CNY/unit) and K_{sff} is the sinking fund factor, whose expression is:

$$K_{sff} = \frac{r}{(1+r)^{Y_i - 1}}, \quad (10)$$

where Y_i is the service life of the i_{th} type of micro-source, with WT and PV having a service life of 20 years, storage batteries having a service life of 1.36 years, and DG having a service life of 10 years.

3.1.4. Fuel cost

The annual fuel cost for the DG as follows:

$$F(t) = aP_{dg}(t) + b\mathrm{P}_{\mathrm{dg,max}}, \tag{11}$$

where $F(t)$ is the generator's fuel consumption at time t, L/h; a and b are the intercept coefficient and slope, with a value of 0.08415 L/kWh for a and 0.246 L/kWh for b; $\mathrm{P}_{\mathrm{dg,max}}$ is the maximum power of the DG, and $P_{dg}(t)$ is the actual operating power of the DG at time t , kW.

$$C_{fuel} = \sum_{t=1}^{8760} K_{fuel} F(t), \tag{12}$$

where K_{fuel} is the price of diesel, which is 8.38 CNY/L.

3.1.5. Environmental cost

Environmental costs are typically not included in traditional economic costs, but they are an essential concept in the theory and practice of sustainable development. The mathematical function representing environmental costs is as follows:

$$C_{pol} = \int_0^T \sum_{i=1}^{3} V_i K_i^{\gamma} P_{dg}(t) dt, \tag{13}$$

where V_i is the treatment cost per kilogram for the i_{th} type of pollutant gas emission, K_i^{γ} is the emission coefficient for the i_{th} type of pollutant gas.

3.2. Constraints

In optimization problems, setting multiple constraints ensures that the solutions are not only mathematically feasible but also meet the requirements of real-world applications. Constraints limit the range of values for decision variables, ensuring that solutions satisfy specific technical, economic, environmental, and other relevant criteria.

3.2.1. Distributed generation output constraints

For any given time t, the output of the i_{th} distributed energy resource must satisfy its maximum output constraint:

$$P_i(t) \leq X^i p_i, \tag{14}$$

where p_i is the individual capacity of a distributed energy resource unit.

3.2.2. Energy storage system operation constraints

Energy storage system operation constraints refer to the limitations and requirements that must be considered when designing and operating an energy storage system within an electrical grid or standalone application. The mathematical expressions for these constraints are as follows:

$$\begin{cases} \mathrm{SOC}_{\min} \leq SOC \leq \mathrm{SOC}_{\max}, \\ P_{ch}(t) \leq 0.2E_s/\Delta t, \\ P_{dch}(t) \leq 0.2E_s/\Delta t \end{cases} \tag{15}$$

where $\mathrm{SOC}_{\min}$ is the minimum capacity of the battery, $\mathrm{SOC}_{\max}$ is the maximum capacity of the battery, $P_{ch}(t)$ and $P_{dch}(t)$ represent the charging and discharging power of the battery, Δt is set to 1 hour.

3.2.3. Power balance constraint

The power balance constraint is a critical aspect of operating an energy storage system. It ensures that the total power supplied to the system is equal to the total power consumed or discharged from the system at any given time. This constraint is essential for maintaining the stability and reliability of the electrical system. The power balance constraint can be expressed as:

$$P_L(t) = P_1(t) + P_2(t) + P_3(t) + P_4(t) + P_{bre}(t), \tag{16}$$

where $P_L(t)$ is the load power; $P_1(t)$, $P_2(t)$, $P_3(t)$ and $P_4(t)$ are the output powers of the PV panels, WTs, BESS, and DGs, respectively $P_{bre}(t)$ is the power shortage.

3.2.4. Power supply reliability constraint

The power shortage at time t in a microgrid can be represented as:

$$P_{bre}(t) = P_L(t) - (P_1(t) + P_2(t) + P_3(t) + P_4(t)) \tag{17}$$

The specific expression for the load interruption rate is:

$$f_{lps} = \sum_{t=1}^{8760} P_{bre}(t) / \sum_{t=1}^{8760} P_L(t) \tag{18}$$

The microgrid must meet a certain level of reliability requirements:

$$f_{lps} \leq f_{\mathrm{lps,\ max}}, \tag{19}$$

where $f_{\text{lps, max}}$ represents the maximum allowable load interruption rate for the microgrid, which is numerically set to 0.1.

3.2.5. Energy waste constraint

The waste power of the microgrid at time t can be represented as:

$$P_{waste}(t) = P_{pv}(t) - P_1(t) - P_5(t) + P_{wt}(t) - P_2(t) - P_6(t) + P_{dg}(t) - P_{dg,was}(t) \tag{20}$$

where $P_{dg,was}(t)$ is the power wasted by the diesel generator when the demand is less than $\mathrm{P_{dg,min}}$, the minimum power output of the diesel generator.

Within a certain period, the ratio of the total wasted power to the total annual load of the system is the energy wastage rate (f_{ewr}), which can be expressed as:

$$f_{ewr} = \sum_{l=1}^{8760} P_{waste}(t) / \sum_{l=1}^{8760} P_L(t) \tag{21}$$

The microgrid must meet a certain level of energy utilization efficiency:

$$f_{ewr} \leq f_{\text{ewr, max}} , \tag{22}$$

where $f_{\text{ewr, max}}$ represents the maximum acceptable energy waste rate for the system, which is numerically set to 0.2.

3.3. Control strategy for microgrid systems

The operation strategy of the hybrid microgrid system adopts a load-following approach [39]. In the wind-solar-battery-diesel microgrid system, wind and PV power generation are significantly affected by environmental conditions and are non-adjustable. BESS can balance power and buffer energy, while DGs and the distribution network serve as supplements and backups for electricity in the system [40]. To improve the economy of the microgrid and ensure its safe and reliable operation, a reasonable operation and control strategy is crucial [41, 42]. The pseudocode of the system operation and control strategy is shown in Algorithm 1.

First, for each time point (every hour of the year), the system checks if PV power generation is sufficient to meet the current load demand. If PV power generation is adequate, it directly supplies the load, and any excess electricity is used to charge the battery. If PV alone cannot meet the load demand but wind power can compensate, wind power is used for supply.

For BESS management, if PV power generation exceeds the load demand, the excess electricity charges the battery. Additionally, if there is still space in the battery, wind power can also be used for charging. If PV and wind power are insufficient to meet the load, the battery discharges to make up the difference.

If the combination of PVs, WTs, and BESS is still insufficient to meet the load demand, the DGs start to supply power. If the output of DGs exceeds the demand, there will be wastage. Conversely, if the

Algorithm 1: Fixed logic control strategy for microgrid system

```
for each hour t in 8760 hours do
    if P_pv · η_i ≥ P_L then
        P_1 = P_L/η_i;   P_2 = P_3 = P_4 = 0;
        Battery stores photovoltaic and wind power sequentially based on remaining capacity;
        Update SOC;
    else
        P_1 = P_pv; if P_wt ≥ P_L/η_i then
            P_2 = P_L − P_pv/η_i;
            P_3 = P_4 = P_5 = 0;
            Battery stores wind turbine power based on remaining capacity;
            Update SOC;
        else
            P_2 = P_wt; if SOC(t) ≥ SOC_min then
                Discharge battery; if Battery meets load demand then
                    P_4 = 0;
                else
                    Update SOC; Use DGs; if Required power < P_dg,min then
                        P_4 = P_dg,min;
                    else if Required power > P_dg,max then
                        P_4 = P_dg,max;
                    else
                        P_4 = P_L − P_pv·η_i − P_wt − P_3·η_i;
```

demand exceeds the maximum output of the DGs, there will be an unsatisfied load demand. Throughout the system's operation, continuous updates of the battery's state of charge are necessary to ensure that the battery does not overcharge or over-discharge.

The overall aim is to maximize the use of renewable energy, reduce reliance on fossil fuels, and ensure the stable operation of the energy system. By managing the distribution of different energy sources efficiently, the strategy meets load demands while maintaining battery health and minimizing DG use. This approach allows the system to better adapt to varying energy demand and supply conditions, improving overall energy efficiency and reliability. These advantages make the load-following strategy an ideal choice for the operation and control of microgrid systems.

4. Optimization algorithms for microgrid capacity configuration

Genetic Algorithm (GA) and PSO are well established optimization techniques with their principles extensively documented in the literature. Given the comprehensive coverage of these methods in prior studies, this paper focuses on the detailed description and application of GWO and its enhanced variant-CGWO. By emphasizing these algorithms, the study aims to highlight their advanced capabilities and demonstrate their effectiveness in solving complex optimization problems within the context of hybrid energy systems.

4.1. Principle of GWO

The GWO is a novel group intelligent optimization algorithm inspired by the social hierarchy mechanism and predatory behavior of grey wolf packs in nature [43]. Grey wolf packs have a strict hierarchy, where α is the highest-ranking wolf, β is the subordinate wolf to α, δ obeys the commands of α and β, and the lowest-ranking wolf is called ω. Grey wolf hunting mainly consists of three stages: tracking and approaching the prey; pursuing and surrounding the prey until it stops moving; and attacking the prey. Assuming there are wolves in the pack, the position of the wolves is X, the best solution in the group is α, the second-best solution is β, the third-best solution is δ, and the other individuals are ω. The mathematical model describing the grey wolf's predatory behavior is as follows [44]:

$$D = \left| C \cdot X_p(t) - X(t) \right|, \tag{23}$$

$$X(t+1) = X_p(t) - A \cdot D, \tag{24}$$

where t represents the current iteration number, A and C are coefficient vectors, and $X_p(t)$ is the position vector of the prey.

$$A = 2a \cdot r_1 - a, \tag{25}$$

$$C = 2 \cdot r_2, \tag{26}$$

where r_1 and r_2 are random vectors within the range [0, 1], a is the convergence factor, and the positions of the other grey wolves in the population are determined collectively by the positions of α, β, and δ:

$$\begin{cases} D_\alpha = |C_1 \cdot X_\alpha - X| \\ D_\beta = |C_2 \cdot X_\beta - X| \\ D_\delta = |C_3 \cdot X_\delta - X| \end{cases} \tag{27}$$

$$\begin{cases} X_1 = X_\alpha - A_1 \cdot D_\alpha \\ X_2 = X_\beta - A_2 \cdot D_\beta \\ X_3 = X_\delta - A_3 \cdot D_\delta \end{cases} \tag{28}$$

$$X(t+1) = \frac{X_1 + X_2 + X_3}{3} \tag{29}$$

4.2. Continuous Grey Wolf optimization

Although the GWO algorithm has demonstrated effectiveness in solving optimization problems due to its simplicity and robustness, it still faces challenges such as low solution accuracy and slow convergence speed, which limit its broader application in engineering optimization. To overcome these shortcomings, the CGWO algorithm was developed as an enhancement of the GWO. This improved algorithm incorporates a convergence factor based on the cosine law to achieve a better balance between global and local search capabilities. Additionally, it introduces a proportional weight update mechanism based on the Euclidean distance of step size, which accelerates the convergence speed. These improvements make the CGWO algorithm a more powerful and efficient tool for addressing the optimization configuration problem of independent microgrid capacity.

4.2.1. Convergence factor with cosine law variation

As known from reference [45], when $|A| > 1$, the grey wolf pack will expand its search range to locate the prey, perform global search, resulting in a faster convergence rate; when $|A| < 1$, the grey wolf pack will contract its search range to attack the prey,

perform local search, leading to a slower convergence rate. Therefore, the size of A is closely related to the global search and local search capabilities of the GWO algorithm. In (25), A changes with the variation of the convergence factor a, which linearly decrements from 2 to 0 with the number of iterations. However, the algorithm's convergence process is not linear throughout its progression. Hence, it is evident that the linearly decrementing convergence factor cannot fully represent the actual optimization search process. Therefore, this paper proposes a convergence factor based on the cosine law variation, whose modified expression is:

$$a = \begin{cases} a_f + (a_i - a_f)\left(1 + \cos\left(\frac{(t-1)\pi}{t_{\max}-1}\right)\right)^n /2, & t \le \frac{1}{2}t_{\max} \\ a_f + (a_i - a_f)\left(1 - \cos\left(\frac{(t-1)\pi}{t_{\max}-1}\right)\right)^n /2, & \frac{1}{2}t_{\max} \le t \le t_{\max} \end{cases} \tag{30}$$

where a_i and a_f represent the initial and final values of the convergence factor a. t is the current iteration number, $t_{\max}$ is the maximum number of iterations, and n is the decremented index, with $0 < n \le 1$. The modified convergence factor forms a curve based on the cosine law variation. It decreases slowly at the beginning of the iteration, allowing the convergence factor a to maintain a larger value for a longer time, thereby extending the duration for which A remains large, which enhances search efficiency. In the later stages of iteration, the decrease is faster, keeping the value of a small for a longer period, extending the duration for which A remains small, thereby improving search accuracy. Therefore, the balance between the algorithm's global search and local search capabilities is achieved.

4.2.2. Introduction of a dynamic weighting strategy

In [46], a proportional weight based on the step size Euclidean distance is proposed, expressed as follows:

$$W_1 = \frac{|X_1|}{|X_1| + |X_2| + |X_3|}, \tag{31}$$

$$W_2 = \frac{|X_2|}{|X_1| + |X_2| + |X_3|}, \tag{32}$$

$$W_3 = \frac{|X_3|}{|X_1| + |X_2| + |X_3|}, \tag{33}$$

$$X(t+1) = \frac{X_1 \cdot W_1 + X_2 \cdot W_2 + X_3 \cdot W_3}{3}, \tag{34}$$

where W_1, W_2 and W_3 represent the learning rates of grey wolf ω towards α, β, and δ wolves. The introduction of the above proportional weights can accelerate the convergence speed of the algorithm.

4.3. Sensitivity analysis

To evaluate the adaptability and robustness of optimization algorithms, a sensitivity analysis was conducted on GA, PSO, GWO, and CGWO under varying population sizes (N=30,60,100,150,250,300). The convergence behaviors of these algorithms are illustrated in Figure 2, revealing distinct performance characteristics for each algorithm.

The parameter settings for all algorithms were kept consistent to ensure a fair comparison. The population size was the same for all algorithms, and the maximum number of iterations was set to 1000. For the GA, the maximum number of generations was capped at 500 to allow sufficient opportunity for convergence, the crossover rate was set at 0.8 to encourage robust genetic recombination, and the mutation rate was set at 0.01 for binary encoding or 0.1 for real-valued encoding to maintain diversity and avoid premature convergence. In the PSO algorithm, the maximum particle velocity V_{max} was set to 5, and both the cognitive coefficient c_1 and the social coefficient c_2 were set to 0.5. For the both CGWO and GWO algorithm, the convergence factor a_i was initialized to 2 and reduced to $a_f = 0$.

The GA algorithm demonstrates the slowest convergence speed and the poorest final solution quality across all tested population sizes. Although it exhibits an initial reduction in the objective function value, the rate of improvement is minimal compared to the other algorithms, and it stagnates early at suboptimal values. These observations highlight GA's inefficiency in balancing global exploration and local exploitation, making it unsuitable for complex optimization tasks. Given its relatively poor performance in convergence speed and solution quality, GA is not considered for further capacity configuration analysis in subsequent sections, as it may not fully meet the requirements of practical engineering applications.

In contrast, PSO achieves faster convergence than GA during the early iterations, leveraging its velocity-based search mechanism to explore the solution space effectively. However, its convergence curves exhibit a distinctive 'staircase' pattern, characterized by periods of slow or minimal improvement in the objective

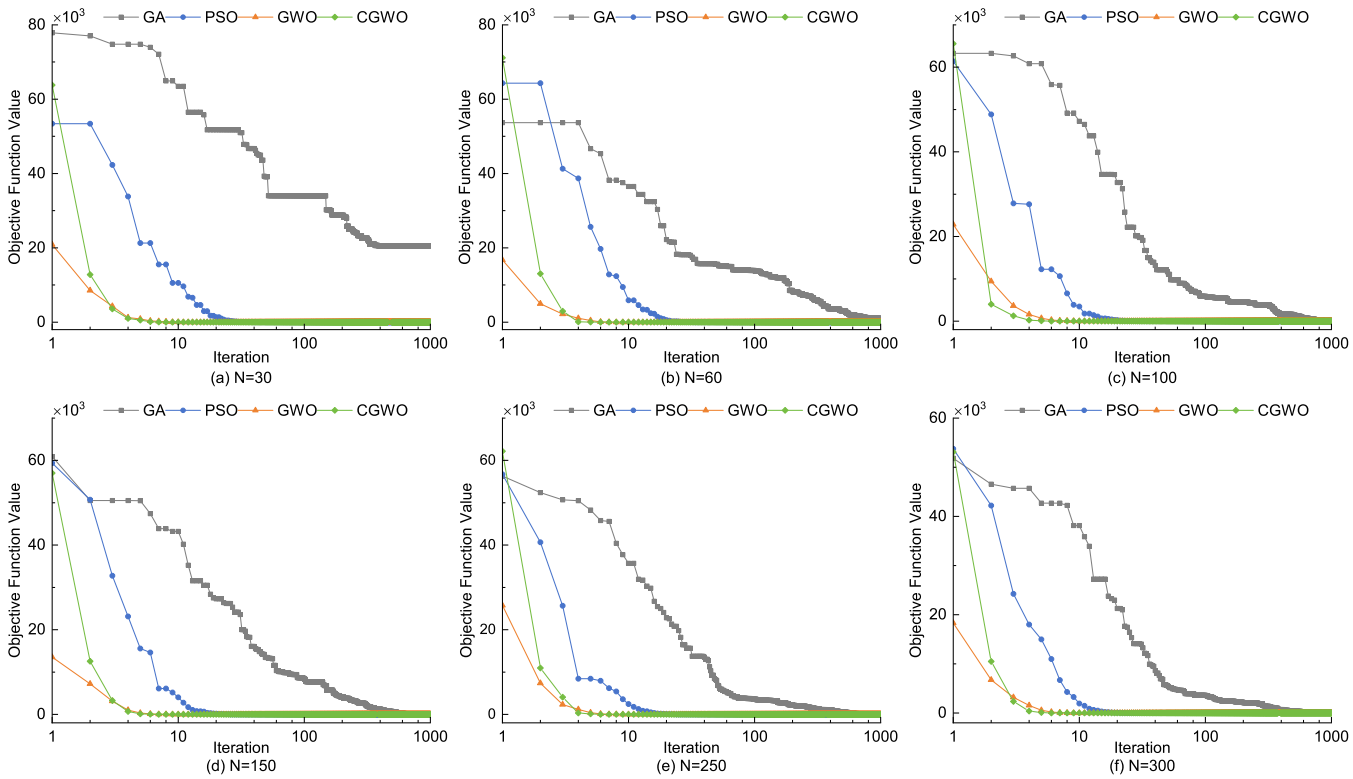

Figure 2: Comparison of varying population sizes under GA, PSO,GWO,and CGWO

function value, followed by sudden decreases when better solutions are found.This behavior indicates that PSO frequently becomes trapped in local optima, with occasional escapes when particles find better solutions. While PSO outperforms GA in terms of speed and accuracy, the staircase phenomenon suggests limited local exploitation capabilities.

GWO, on the other hand, exhibits stable and consistent convergence, outperforming both GA and PSO across all population sizes. Its hierarchical leadership structure and adaptive position updates enable it to achieve a better balance between global and local search, resulting in faster and more reliable optimization. Despite these strengths, GWO's performance is slightly inferior to CGWO.

4.4. Comparative convergence analysis of GWO and CGWO on benchmark functions

The four benchmark functions employed in this study are selected from the CEC2005 test suite, a widely recognized standard for evaluating optimization algorithms. These functions are designed to simulate various real-world challenges, including stochastic disturbances, multimodal landscapes, flat regions, and complex constraints. For instance, the random noise in Function 1 (F1) reflects the stochastic nature of renewable energy generation, while the multimodal landscapes of Functions 2 (F2) and 3 (F3) capture the non-convexity and nonlinearity characteristic of microgrid optimization problems. Additionally, the complexity and penalty terms in Function 4 (F4) align with the multidimensional constraints and trade-offs inherent in microgrid planning and operations. The mathematical formulations and properties of these functions are summarized in Table 1.

The comparative performance of GWO and CGWO on these benchmark functions is presented in Figure 3. Across all test cases, CGWO consistently outperforms GWO in both convergence speed and final solution quality. On F1, a unimodal function with random noise, CGWO achieves faster convergence and demonstrates greater robustness against stochastic disturbances. For F2, a multimodal function with numerous local optima, both CGWO and GWO exhibit periods of stagnation during the optimization process, reflecting the difficulty of escaping the dense local optima characteristic of this function. However, CGWO shows a superior ability to eventually overcome these stagnation phases, achieving faster convergence to the global optimum compared to GWO. This demonstrates CGWO's enhanced ex-

Table 1: Mathematical expressions and search ranges of the benchmark functions used for CGWO and GWO evaluation.

Function	Expression	Search Range
1	$\sum_{i=1}^{n} i \cdot x_i^4 + \text{rand}$	$x_i \in [-1.28, 1.28]$
2	$\sum_{i=1}^{n} \left(x_i^2 - 10\cos(2\pi x_i) + 10\right)$	$x_i \in [-5.12, 5.12]$
3	$-20\exp\left(-0.2\sqrt{\frac{1}{n}\sum_{i=1}^{n} x_i^2}\right) - \exp\left(\frac{1}{n}\sum_{i=1}^{n}\cos(2\pi x_i)\right) + 20 + e$	$x_i \in [-32, 32]$
4	$0.1\left[\sin^2(3\pi x_1) + \sum_{i=1}^{n-1}(x_i-1)^2 \cdot \left(1+\sin^2(3\pi x_{i+1})\right) + (x_n-1)^2\left(1+\sin^2(2\pi x_n)\right)\right] + \sum_{i=1}^{n} U(x_i, 5, 100, 4)$	$x_i \in [-50, 50]$

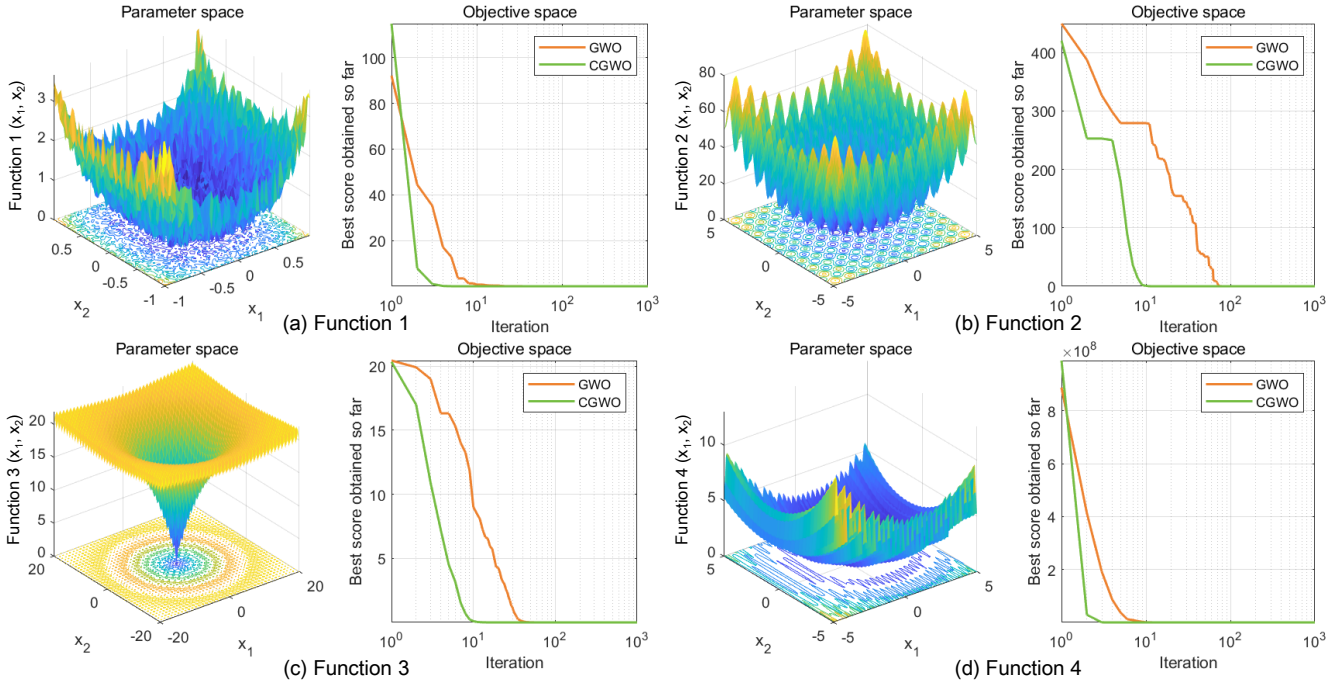

Figure 3: Comparison of GWO and CGWO on benchmark functions

ploration capabilities, although the challenges posed by F2's multimodal landscape still influence both algorithms. On F3, which contains flat regions challenging for gradient-based methods, CGWO converges more efficiently to the global optimum, addressing GWO's limitations in low-gradient scenarios. Finally, for F4, a highly complex multimodal function with penalty terms, CGWO maintains a smoother convergence trajectory and delivers significantly better final solutions, showcasing its adaptability to constrained and complex optimization landscapes.

These results underscore CGWO's superior performance across all benchmark functions, highlighting its effectiveness in tackling challenges such as multimodality, stochastic disturbances, and complex constraints. The enhancements in CGWO, including a cosine-based convergence factor and proportional weight updates, are pivotal to its faster convergence and higher solution accuracy.

4.5. Optimizing microgrid capacity configuration with the CGWO algorithm

In the process of solving the optimization configuration model for an independent microgrid with wind, solar, storage, and diesel, the decision variables for the optimization problem are chosen to be the number of WTs, PV panels, batteries, and DGs, $X = \left(X^{wt}, X^{pv}, X^{b}, X^{dg}\right)$. Through the iteration and optimization of the CGWO algorithm, a set of power capacity configuration solutions with the lowest annual average system cost is obtained under the conditions of meeting the load demand and system con-

straints. The CGWO procedure can be described by the flowchart in Figure 4.

The process is divided into the following stages:

(1) Initialization: The algorithm begins by initializing the population size N, the maximum number of iterations $t_{\max}$, and relevant parameters such as a_i, a_f, A_1, C_1. The initial positions of grey wolf pack X_i contains X^{wt}, X^{pv}, X^b, X^{dg} are randomly generated within the search space.

(2) Fitness Evaluation (Identify the Leader): At each iteration t, the fitness value of each wolf pack $X_i\,(i \in [1, N])$ using Equation (5), which represent the C_{all} are calculated. Based on these values, the three best-performing wolves, X_α, X_β, and X_γ, are identified as the leading wolves representing the current optimal solutions.

(3) Position Update (Hunting): The hunting process begins by calculating the distances D_α, D_β, and D_γ from the current positions of the leading wolves to the prey (target position) using Equation (27). Subsequently, the three candidate positions X_1, X_2, and X_3 are computed using Equation (28).

(4) CGWO Improvement: To enhance convergence performance, weighted factors W_1, W_2, and W_3 are introduced in (31)–(33). These weights balance the influence of the three leading wolves, and the updated position $X(t+1)$ is derived using Equation (34).

(5) Parameter Update: The control parameters A and C are updated for the next iteration according to Equations (25) and (26), ensuring adaptive exploration and exploitation during the optimization process.

(6) Termination and Output: The iteration continues until the maximum iteration count $t_{\max}$ is reached. At this point, the algorithm outputs the best grey wolf pack position $X(t+1)$, representing the optimal capacity configuration solution.

By following these steps, the CGWO algorithm can effectively search for the optimal microgrid capacity configuration that meets the requirements, balancing economic efficiency and reliability.

5. Case study

The objective is to design an isolated hybrid energy system for an integrated park. Based on one year of meteorological data from an integrated park in a specific region and the actual electricity consumption over the same period, the CGWO algorithm proposed in this study is utilized to optimize the capacity of an independent microgrid. The data sampling interval is one hour, including wind speed, irradiance, and load data for the entire year, totalling 8,760 hours. These parameters are illustrated in Figure 5. The total annual electricity consumption in the area amounts to 884.14 MWh, with an average daily consumption of approximately 2.42 MWh. Table 2 presents the technical and economic parameters of different devices, sourced from [47].

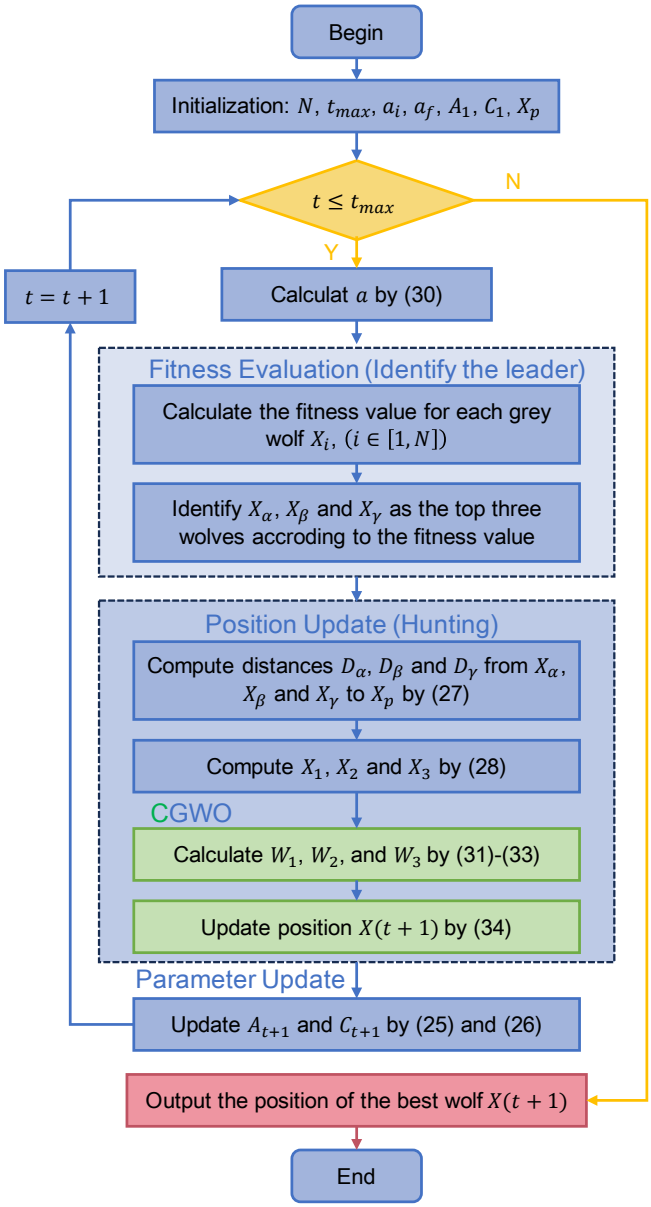

Figure 4: Capacity configuration process under CGWO algorithm

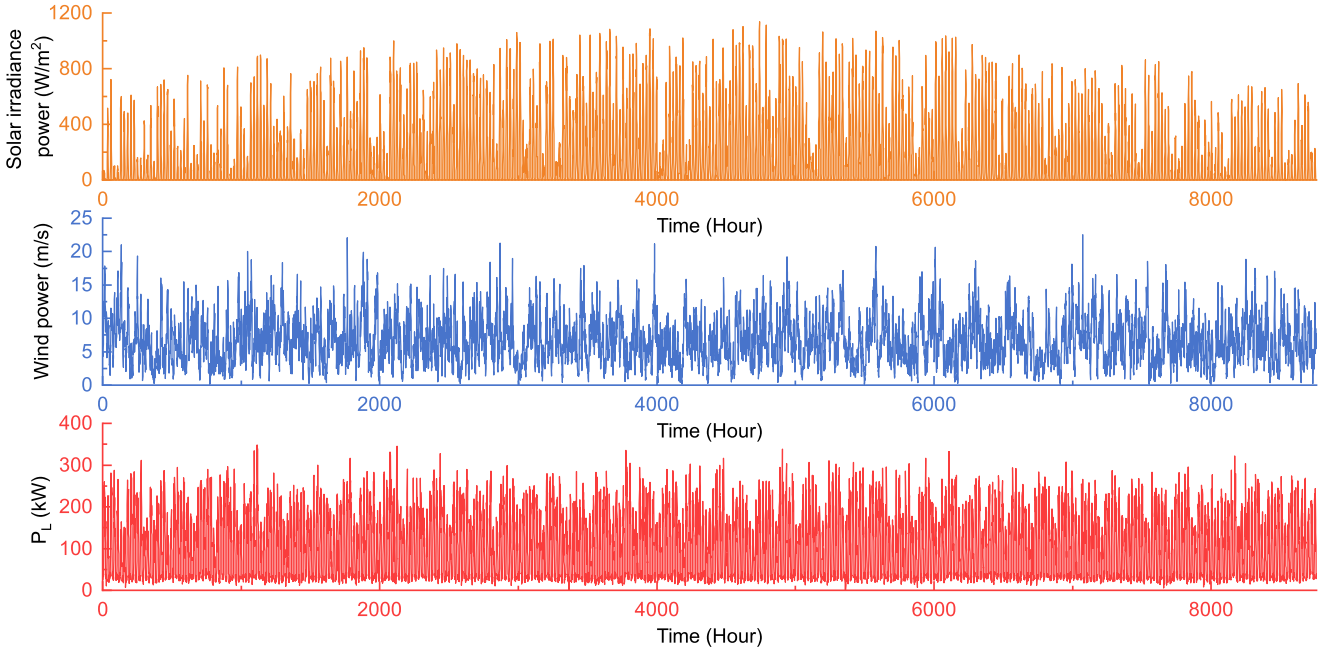

Figure 5: Annual hourly solar irradiance, wind speed, and electricity load

5.1. *Performance analysis of hybrid microgrid power supply schemes*

To analyze and compare the impact of different power hybrid schemes on the economy of standalone microgrids, four distinct microgrid power supply combination schemes were established. These schemes comprise WTs, PVs, BESS, and DGs, are detailed in Table 3.

The optimization problem of microgrid power capacity configuration under these four schemes is solved using the CGWO algorithm, programmed in Matlab software. The parameters for the CGWO algorithm are set as follows: population size N is 150, $t_{\max}$ is 250, and the dimension of position is 4.

Table 4 compares the optimal configuration results across various hybrid energy systems, while Figure 6 illustrates the detailed capacity configurations under different schemes. As shown in Figure 6, Scheme 4 incurs significantly higher total costs and environmental conversion expenses than Schemes 1, 2, and 3. Among these, Scheme 3 achieves the lowest total cost and environmental conversion expenses. Specifically, compared to Scheme 1, Scheme 3 reduces total costs by 30.12% and environmental conversion expenses by 59.7%; compared to Scheme 2, it achieves savings of 16.74% in total costs and 39.84% in environmental conversion expenses.

Figure 6 highlights the superior performance of Scheme 3, optimized by the CGWO algorithm, in minimizing environmental expenses and meeting sustainability goals. This ensures cost control while reliably fulfilling energy demands, positioning Scheme 3 as a sustainable solution. Furthermore, Scheme 3 significantly reduces load-shedding rates, enhancing reliability and renewable energy utilization by decreasing dependence on diesel generators and batteries. Despite higher initial investment, it benefits from lower operational and environmental costs, ensuring long-term economic and social advantages. This configuration offers a strategic, sustainable framework for microgrid optimization in remote areas.

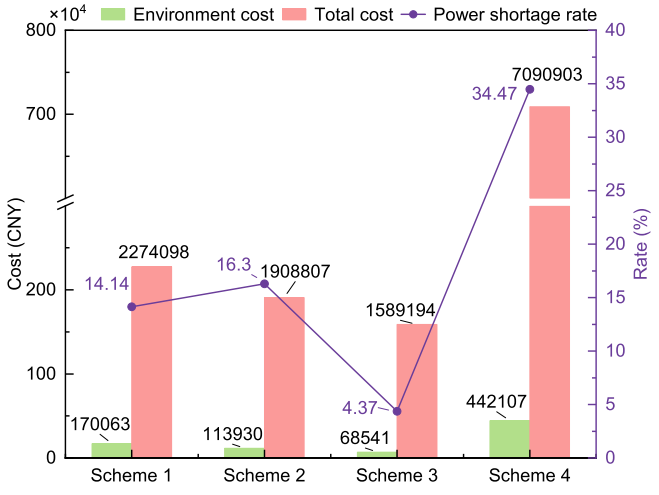

Figure 6: Comparison of optimal sizing results for different hybrid energy systems

Table 2: Technical and economical parameters.

Variable	Value	Unit
a	0.08415	L/kWh
b	0.246	L/kWh
c_{dis}	1.0	—
c_{cha}	0.8	—
E_s	2	kWh
G_n	1000	W/m^2
k_{dg}	500	CNY/year
k_{fuel}	8.38	CNY/L
k_{pv}	20	CNY/year
k_s	20	CNY/year
k_{wt}	200	CNY/year
$kr_{\mathrm{CO_2}}$	649	g/kWh
kr_{NO_x}	9.890	g/kWh
$kr_{\mathrm{SO_2}}$	0.206	g/kWh
P_{wt}	35	kW
P_{pv}	1	kW
$\mathrm{P_{dg,max}}$	50	kW
$\mathrm{P_{dg,min}}$	10	kW
$\mathrm{P_{cha,max}}$	$0.2 \times E_s$	kW
$\mathrm{P_{dis,max}}$	$0.2 \times E_s$	kW
R_{wt}	30000	CNY/unit
R_{pv}	7000	CNY/unit
R_{dg}	1800	CNY/unit
R_s	900	CNY/unit
r	0.0475	%
$\mathrm{SOC_{max}}$	0.9	—
$\mathrm{SOC_{min}}$	0.2	—
T_r	25	℃
u_{wt}	18600	CNY/unit
u_{pv}	10000	CNY/unit
u_{de}	2390	CNY/unit
u_s	1600	CNY/unit
v_{ci}	3	m/s
v_{co}	25	m/s
v_n	11	m/s
$V_{\mathrm{CO_2}}$	0.210	CNY/kg
$V_{\mathrm{SO_2}}$	14.842	CNY/kg
V_{NO_x}	62.964	CNY/kg
Y	20	year
Y_{de}	10	year
Y_s	1.36	year
λ	-0.0047	%

Table 3: Comparison of optimal sizing results for different hybrid energy systems

Scheme	WT	PV	BESS	DG
1		✓	✓	✓
2	✓		✓	✓
3	✓	✓	✓	✓
4			✓	✓

5.2. Comparative analysis of CGWO and other algorithms

To further validate the effectiveness of the CGWO algorithm in optimizing the capacity configuration of wind-solar-battery-diesel microgrid systems, we applied the CGWO, GWO, and PSO algorithms to solve the power capacity optimization problem under Scheme 3.

Table 4: Comparison of optimal sizing results for different hybrid energy systems

Scheme	X^{wt}	X^{pv}	X^b	X^{dg}
1	0	619	23	1
2	7	0	19	1
3	5	500	15	1
4	0	0	25	2

Table 5 offers a comparative analysis of the optimal capacity configurations achieved by the CGWO, GWO, and PSO algorithms. The results presented in Figure 7 reveal that the microgrid costs under the CGWO algorithm are the lowest among the three, including both fuel costs and environmental management costs. The cost savings achieved by the CGWO algorithm are approximately 2.73% compared to the GWO algorithm and approximately 4.16% compared to the PSO algorithm, underscoring its superior economic efficiency.

Table 5: Comparison of CGWO,GWO and PSO

Algorithm	X^{wt}	X^{pv}	X^b	X^{dg}	Total cost(CNY)
CGWO	5	100	15	1	1,589,194
GWO	4	546	15	1	1,633,772
PSO	4	560	20	1	1,658,163

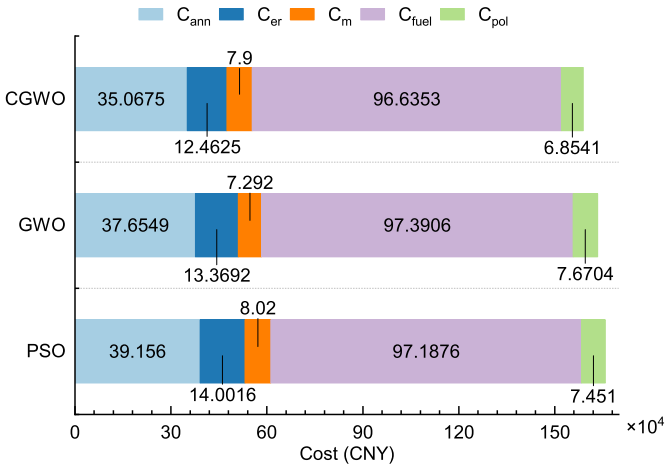

Figure 7: Cost composition under CGWO,GWO and PSO

For the design of an independent hybrid power system to provide the necessary energy for integrated park facilities, data from two consecutive days (one

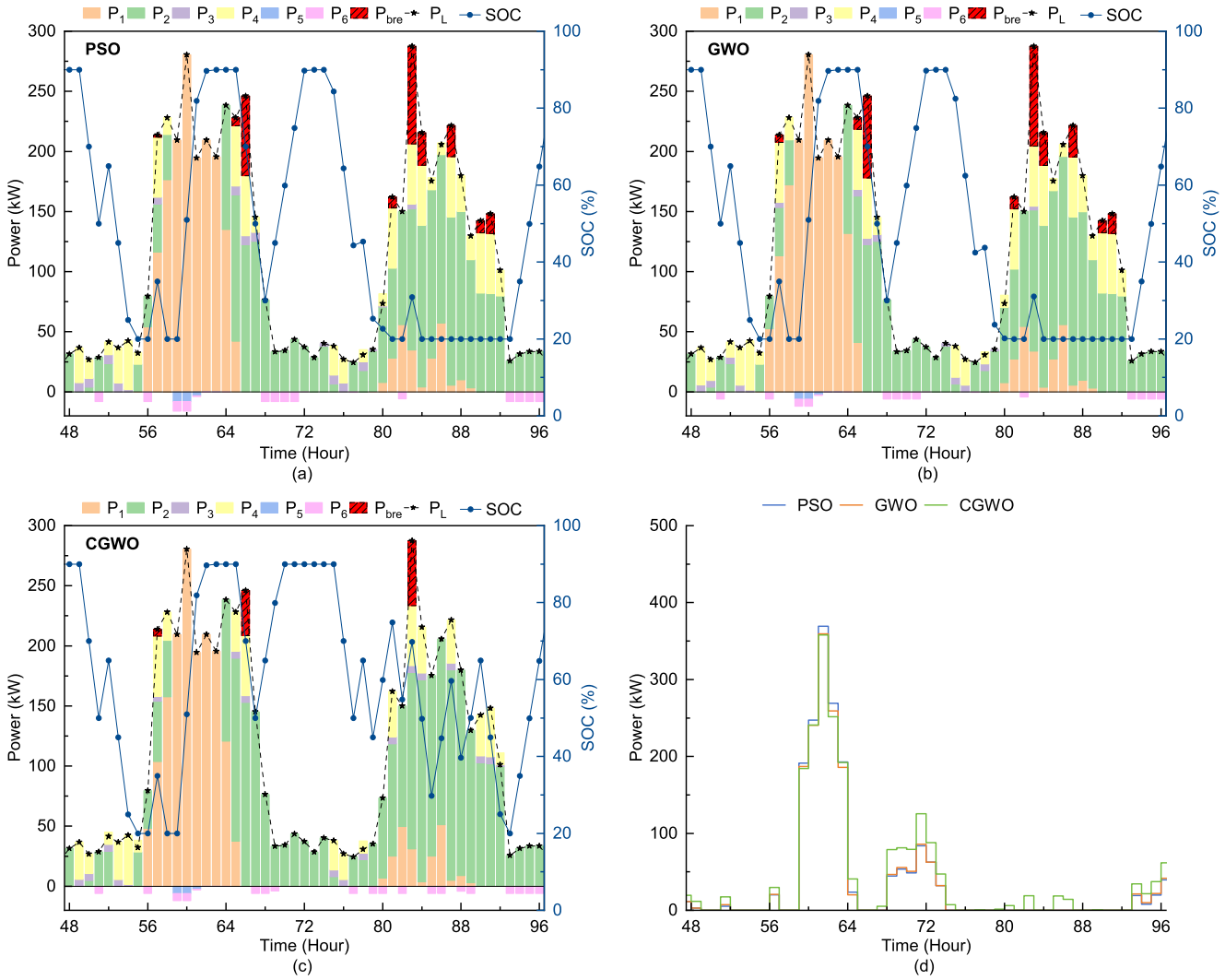

Figure 8: Comparison of optimal sizing results using CGWO, GWO and PSO

sunny and one cloudy) in a year were selected for analysis. Figures 8 (a)-(d) show the comparative analysis of the PSO, GWO, and CGWO algorithms, In these figures, P_1 represents the PVs output supply to the load, P_2 is the WTs output supply to the load, P_3 is the batteries supply to the load, P_4 is the DGs supply to the load, P_5 is the PVs output for battery charging, P_6 is the WTs output for battery charging, P_{bre} is the power shortage, P_L is the actual load, and SOC is the state of charge.

Wind-solar complementarity: The wind and solar power output configurations calculated by the three algorithms leverage the complementary nature of wind and solar energy. When light intensity is high, the systems predominantly rely on PV power generation, while wind power generation becomes the primary source under low light conditions. This demonstrates the advantages of wind-solar complementarity in balancing energy supply. Among the algorithms, the CGWO achieves the most robust configuration by allocating the largest number of wind turbines , enabling it to better meet load demands during periods without sunlight. As illustrated in the red histogram in Figure 8, the power shortages for the CGWO, GWO, and PSO algorithms are 97.38 kW, 256.84 kW, and 244.96 kW, respectively, highlighting the superior performance of the CGWO algorithm in minimizing power deficits.

Performance of BESS: The operation patterns of the BESS exhibit similarities across the three algorithms under optimal light conditions, with comparable charging and discharging behaviors. However, during prolonged periods of low light intensity (75 to 92 hours), the CGWO algorithm demonstrates supe-

rior performance. The BESS effectively operates as both a storage and output device, efficiently storing surplus wind power to address the issue of "curtailed wind" and ensuring that generated energy is utilized rather than wasted. Additionally, the CGWO-managed BESS reliably supplies power during demand periods, enhancing system efficiency and stability.

In contrast, the BESS performance under the PSO and GWO algorithms is less effective, with limited utilization of the battery's storage capacity. This underutilization reflects a suboptimal approach to energy management, underscoring the advantages of the CGWO algorithm in maximizing the potential of energy storage systems.

Diesel generator utilization: The DGs output demonstrates significant differences across the three algorithms. With its robust configuration of wind turbines, the CGWO algorithm effectively minimizes reliance on DGs, particularly during peak demand periods when PV output is unavailable. This efficient utilization of renewable energy sources reduces the dependency on fossil fuel-based power generation.

As a result, the DG outputs under the CGWO, GWO, and PSO algorithms are 597.92 kW, 784.48 kW, and 766.2 kW, respectively, highlighting the superior performance of the CGWO algorithm in reducing diesel generator usage and promoting a more sustainable energy mix.

Clean energy utilization: Figure 8 (d) highlights the waste of clean energy power under different weather conditions. On sunny days, both PV and wind power generation may experience some energy waste, with the PSO algorithm showing the highest waste due to its increased number of photovoltaic panels. Conversely, on cloudy days, the CGWO algorithm exhibits higher energy waste, attributed to its larger number of wind turbines.

Nevertheless, a comprehensive two-day analysis reveals that while the CGWO algorithm increases clean energy waste by 16.53% and 15.01% compared to the GWO and PSO algorithms, respectively, it achieves substantial improvements in other performance metrics. The power shortage rate decreases by 62.09% and 60.25%, and reliance on DGs reduces by 23.78% and 22.04%, respectively.

This trade-off significantly enhances the system's ability to meet load demands during periods of low solar irradiance, improves reliability, reduces power shortages, and achieves the lowest total cost. These benefits position the CGWO algorithm as a highly economic and efficient solution for microgrid capacity optimization, balancing renewable energy utilization with system performance and cost-effectiveness.

6. Conclusions

This study presents an innovative optimization framework for the capacity configuration of hybrid microgrid systems, incorporating wind turbines (WT), photovoltaic (PV) panels , battery energy storage systems (BESS), and diesel generators (DG). The proposed Continuous Grey Wolf Optimization (CGWO) algorithm enhances the traditional GWO by introducing a cosine-law-based convergence factor and a dynamic weighting strategy. These improvements significantly enhance the algorithm's ability to balance global exploration and local exploitation, resulting in faster convergence and higher solution accuracy.

Benchmark testing on standard CEC2005 functions validates CGWO's robustness and adaptability. The algorithm consistently outperforms the original GWO, demonstrating its capability to handle multimodal landscapes, stochastic disturbances, and flat regions characteristic of real-world optimization problems. These results underline the importance of advanced optimization techniques for addressing complex engineering challenges.

Four hybrid power supply schemes were assessed for microgrid capacity configuration using the CGWO algorithm. Scheme 3 (WT-PV-BESS-DG) emerges as the most cost-effective option, achieving the lowest total cost and environmental expenses. Compared to Scheme 1, Scheme 3 reduces total costs by 30.12% and environmental expenses by 59.7%, while achieving significant improvements in reliability and renewable energy utilization. Additionally, the CGWO algorithm demonstrates superior performance over GWO and PSO in this application. Specifically, CGWO reduces diesel generator usage by 23.78% and 22.04%, and power shortages by 62.09% and 60.25%, compared to GWO and PSO, respectively. In terms of total annual costs, CGWO achieves savings of 2.73% and 4.16% compared to GWO and PSO, respectively. These findings demonstrate CGWO's capability to optimize microgrid configurations, balancing cost, sustainability, and reliability.

Future research will focus on the impact of varying environmental policies and market conditions on the algorithm's performance, offering deeper insights into its adaptability and robustness. Furthermore,

examining the allocation and constraints of active and reactive power during significant disturbances could provide valuable strategies for ensuring microgrid stability under extreme conditions.

CRediT authorship contribution statement

Zhiling Ren: Writing - Original Draft. Qinwen Yu: Writing - Software. Dong Lin: Review & Editing, Supervision. Yun Dong: Review & Editing, Supervision.

Declaration of competing interest

The authors declare that they have no known competing financial interests or personal relationships that could have appeared to influence the work reported in this paper.

Declaration of using artificial intelligence (AI)

During the preparation of this work, the authors used ChatGPT for language refinement and grammatical corrections. After using this tool, the authors reviewed and edited the content as needed and take full responsibility for the content of the publication.

Acknowledgements

This work is supported by the Liaoning Province Research Project (Grant No. JYTQN2023197) and the University-local government scientific and technical cooperation cultivation project of Ordos Institute-LNTU(Grant No.YJY-XD-2023-04).

References

[1] G. Mutezo, J. Mulopo, A review of Africa's transition from fossil fuels to renewable energy using circular economy principles, Renewable and Sustainable Energy Reviews 137 (2021) 110609.

[2] M. M. Kamal, I. Ashraf, E. Fernandez, Planning and optimization of microgrid for rural electrification with integration of renewable energy resources, Journal of Energy Storage 52 (2022) 104782.

[3] S. Jin, S. Wang, F. Fang, Game theoretical analysis on capacity configuration for microgrid based on multi-agent system, International Journal of Electrical Power & Energy Systems 125 (2021) 106485.

[4] N. Dougier, P. Garambois, J. Gomand, L. Roucoules, Multi-objective non-weighted optimization to explore new efficient design of electrical microgrids, Applied Energy 304 (2021) 117758.

[5] D. Zhang, G. Shafiullah, C. K. Das, K. W. Wong, A systematic review of optimal planning and deployment of distributed generation and energy storage systems in power networks, Journal of Energy Storage 56 (2022) 105937.

[6] D. Yang, C. Jiang, G. Cai, D. Yang, X. Liu, Interval method based optimal planning of multi-energy microgrid with uncertain renewable generation and demand, Applied Energy 277 (2020) 115491.

[7] A. Amiruddin, A. Liebman, R. Dargaville, R. Gawler, Optimal energy storage configuration to support 100% renewable energy for indonesia, Energy for Sustainable Development 81 (2024) 101509.

[8] C. Wang, Z. Zhang, O. Abedinia, S. G. Farkoush, Modeling and analysis of a microgrid considering the uncertainty in renewable energy resources, energy storage systems and demand management in electrical retail market, Journal of Energy Storage 33 (2021) 102111.

[9] C. S. Lai, G. Locatelli, Economic and financial appraisal of novel large-scale energy storage technologies, Energy 214 (2021) 118954.

[10] T. B. Nkwanyana, M. W. Siti, Z. Wang, I. Toudjeu, N. T. Mbungu, W. Mulumba, An assessment of hybrid-energy storage systems in the renewable environments, Journal of Energy Storage 72 (2023) 108307.

[11] P. Puranen, A. Kosonen, J. Ahola, Techno-economic viability of energy storage concepts combined with a residential solar photovoltaic system: A case study from finland, Applied Energy 298 (2021) 117199.

[12] P. Huang, Y. Sun, M. Lovati, X. Zhang, Solar-photovoltaic-power-sharing-based design optimization of distributed energy storage systems for performance improvements, Energy 222 (2021) 119931.

[13] M. S. Nazir, A. N. Abdalla, Y. Wang, Z. Chu, J. Jie, P. Tian, M. Jiang, I. Khan, P. Sanjeevikumar, Y. Tang, Optimization configuration of energy storage capacity based on the microgrid reliable output power, Journal of Energy Storage 32 (2020) 101866.

[14] A. A. Z. Diab, A. M. El-Rifaie, M. M. Zaky, M. A. Tolba, Optimal sizing of stand-alone microgrids based on recent metaheuristic algorithms, Mathematics 10 (1) (2022) 140.

[15] S. Ayachi, X. He, H. J. Yoon, Solar thermoelectricity for power generation, Advanced Energy Materials 13 (28) (2023) 2300937.

[16] J. Guerrero, D. Gebbran, S. Mhanna, A. C. Chapman, G. Verbič, Towards a transactive energy system for integration of distributed energy resources: Home energy management, distributed optimal power flow, and peer-to-peer energy trading, Renewable and Sustainable Energy Reviews 132 (2020) 110000.

[17] S. A. Mansouri, A. Ahmarinejad, E. Nematbakhsh, M. S. Javadi, A. R. Jordehi, J. P. Catalao, Energy management in microgrids including smart homes: A multi-objective approach, Sustainable Cities and Society 69 (2021) 102852.

[18] A. Nawaz, M. Zhou, J. Wu, C. Long, A comprehensive review on energy management, demand response, and coordination schemes utilization in multi-microgrids network, Applied Energy 323 (2022) 119596.

[19] A. L. Bukar, C. W. Tan, L. K. Yiew, R. Ayop, W.-S. Tan, A rule-based energy management scheme for long-term optimal capacity planning of grid-independent microgrid optimized by multi-objective grasshopper optimization al-

gorithm, Energy Conversion and Management 221 (2020) 113161.
[20] X. Chen, W. Dong, Q. Yang, Robust optimal capacity planning of grid-connected microgrid considering energy management under multi-dimensional uncertainties, Applied Energy 323 (2022) 119642.
[21] F. S. Gharehchopogh, M. Namazi, L. Ebrahimi, B. Abdollahzadeh, Advances in sparrow search algorithm: a comprehensive survey, Archives of Computational Methods in Engineering 30 (1) (2023) 427–455.
[22] C. Yang, W. Ye, Q. Li, Review of the performance optimization of parallel manipulators, Mechanism and Machine Theory 170 (2022) 104725.
[23] A. R. Yildiz, H. Abderazek, S. Mirjalili, A comparative study of recent non-traditional methods for mechanical design optimization, Archives of Computational Methods in Engineering 27 (4) (2020) 1031–1048.
[24] A. Almadhor, H. T. Rauf, M. A. Khan, S. Kadry, Y. Nam, A hybrid algorithm (BAPSO) for capacity configuration optimization in a distributed solar PV based microgrid, Energy Reports 7 (2021) 7906–7912.
[25] M. A. Hossain, H. R. Pota, S. Squartini, A. F. Abdou, Modified pso algorithm for real-time energy management in grid-connected microgrids, Renewable Energy 136 (2019) 746–757.
[26] G. K. Suman, J. M. Guerrero, O. P. Roy, Optimisation of solar/wind/bio-generator/diesel/battery based microgrids for rural areas: A PSO-GWO approach, Sustainable Cities and Society 67 (2021) 102723.
[27] A. X. Y. Mah, W. S. Ho, M. H. Hassim, H. Hashim, G. H. T. Ling, C. S. Ho, Z. Ab Muis, Optimization of a standalone photovoltaic-based microgrid with electrical and hydrogen loads, Energy 235 (2021) 121218.
[28] A. Alzahrani, M. A. Hayat, A. Khan, G. Hafeez, F. A. Khan, M. I. Khan, S. Ali, Optimum sizing of stand-alone microgrids: Wind turbine, solar photovoltaic, and energy storage system, Journal of Energy Storage 73 (2023) 108611.
[29] A. Cagnano, E. De Tuglie, P. Mancarella, Microgrids: Overview and guidelines for practical implementations and operation, Applied Energy 258 (2020) 114039.
[30] W. Jiang, X. Wang, H. Huang, D. Zhang, N. Ghadimi, Optimal economic scheduling of microgrids considering renewable energy sources based on energy hub model using demand response and improved water wave optimization algorithm, Journal of Energy Storage 55 (2022) 105311.
[31] J. Yang, C. Su, Robust optimization of microgrid based on renewable distributed power generation and load demand uncertainty, Energy 223 (2021) 120043.
[32] M. H. Nadimi-Shahraki, S. Taghian, S. Mirjalili, H. Zamani, A. Bahreininejad, Ggwo: Gaze cues learning-based grey wolf optimizer and its applications for solving engineering problems, Journal of Computational Science 61 (2022) 101636.
[33] B. Bacha, H. Ghodbane, H. Dahmani, A. Betka, A. Toumi, A. Chouder, Optimal sizing of a hybrid microgrid system using solar, wind, diesel, and battery energy storage to alleviate energy poverty in a rural area of Biskra, Algeria, Journal of Energy Storage 84 (2024) 110651.
[34] J. Mishra, P. K. Behera, M. Pattnaik, B. C. Babu, A multi-agent petri net model power management strategy for wind–solar-battery driven DC microgrid, Sustainable Energy Technologies and Assessments 55 (2023) 102859.
[35] S. Pannala, N. Patari, A. K. Srivastava, N. P. Padhy, Effective control and management scheme for isolated and grid connected dc microgrid, IEEE Transactions on Industry Applications 56 (6) (2020) 6767–6780.
[36] W. Wang, K. Chen, Y. Bai, Y. Chen, J. Wang, New estimation method of wind power density with three-parameter weibull distribution: A case on central inner mongolia suburbs, Wind Energy 25 (2) (2022) 368–386.
[37] M. Wahbah, S. Feng, T. H. El-Fouly, B. Zahawi, Root-transformed local linear regression for solar irradiance probability density estimation, IEEE Transactions On Power Systems 35 (1) (2019) 652–661.
[38] A. Jani, H. Karimi, S. Jadid, Hybrid energy management for islanded networked microgrids considering battery energy storage and wasted energy, Journal of Energy Storage 40 (2021) 102700.
[39] G. Gust, T. Brandt, S. Mashayekh, M. Heleno, N. DeForest, M. Stadler, D. Neumann, Strategies for microgrid operation under real-world conditions, European Journal of Operational Research 292 (1) (2021) 339–352.
[40] C. Yan, J. Chen, H. Liu, L. Kumar, H. Lu, Health management for pem fuel cells based on an active fault tolerant control strategy, IEEE Transactions on Sustainable Energy 12 (2) (2020) 1311–1320.
[41] S. Abulanwar, A. Ghanem, M. E. Rizk, W. Hu, Adaptive synergistic control strategy for a hybrid AC/DC microgrid during normal operation and contingencies, Applied Energy 304 (2021) 117756.
[42] S. Choudhury, Review of energy storage system technologies integration to microgrid: Types, control strategies, issues, and future prospects, Journal of Energy Storage 48 (2022) 103966.
[43] S. Mirjalili, S. M. Mirjalili, A. Lewis, Grey wolf optimizer, Advances In Engineering Software 69 (2014) 46–61.
[44] S. Saremi, S. Z. Mirjalili, S. M. Mirjalili, Evolutionary population dynamics and grey wolf optimizer, Neural Computing and Applications 26 (2015) 1257–1263.
[45] M. H. Nadimi-Shahraki, S. Taghian, S. Mirjalili, An improved grey wolf optimizer for solving engineering problems, Expert Systems with Applications 166 (2021) 113917.
[46] S. Mirjalili, S. Saremi, S. M. Mirjalili, L. d. S. Coelho, Multi-objective grey wolf optimizer: a novel algorithm for multi-criterion optimization, Expert Systems With Applications 47 (2016) 106–119.
[47] A. Malheiro, P. M. Castro, R. M. Lima, A. Estanqueiro, Integrated sizing and scheduling of wind/PV/diesel/battery isolated systems, Renewable Energy 83 (2015) 646–657.